Solutions of (7), and (4) yields

$$\frac{Z_{in}}{Z(l)}=\frac{Z_a\left[\frac{1}{\lambda_g}-\frac{1}{\lambda_c}\tan\frac{2\pi l}{\lambda_g}\right]+j\frac{Z_1}{\lambda}\tan\left(\frac{2\pi l}{\lambda_g}\right)}{Z_1\left[\frac{1}{\lambda_g}+\frac{1}{\lambda_c}\tan\frac{2\pi l}{\lambda_g}\right]+j\frac{Za}{\lambda}\tan\left(\frac{2\pi l}{\lambda_g}\right)} \quad (8)$$

where

$$\lambda_g=\frac{\lambda}{\sqrt{1-\left(\frac{\lambda}{\lambda c}\right)^2}}$$

$$\lambda_c=4\pi L\ln(Z_1/Z_2).$$

IV. Cosine-Squared Tapered Line

In this case impedance of the transmission line varies with position also, and at a distance l from the load

$$Z=a\cos^2 bl \quad (9)$$

when

$$l=0,\ Z(0)=Z_1=a$$

$$l=L,\ Z(L)=Z_2=Z_1\cos^2 bL$$

$$b=\frac{1}{L}\cos^{-1}\frac{Z_2}{Z_1}.$$

From (5) and (9)

$$\frac{d^2u}{dl^2}+(-2b\tan bl)\frac{du}{dl}+\beta^2u=0. \quad (10)$$

Solution of (10) by following [12], and using (4)

$$\frac{Z_{in}}{Z(l)}=\sqrt{1+\left(\frac{b}{\beta}\right)^2}\cdot\left[\frac{Z_a+j\left\{\sqrt{1+\left(\frac{b}{\beta}\right)^2}\right\}Z_1\tan l\sqrt{\beta^2+b^2}}{Z_1\sqrt{1+\left(\frac{b}{\beta}\right)^2}+jZ_a\tan l\sqrt{\beta^2+b^2}}\right]-j\frac{b}{\beta}\tan bl. \quad (11)$$

V. Parabolic Taper

In this section input impedance Z_{in} of a parabolic tapered transmission line terminated in load Z_a is presented. Impedance of the transmission line varies with position l

$$Z=(a+bl)^2 \quad (12)$$

when $l=0$

$$Z(0)=Z_1=a^2$$

when $l=L$

$$Z(L)=Z_2=(a+bL)^2.$$

Therefore, $b=(\pm\sqrt{Z_2}\mp\sqrt{Z_1})/L$. From (5) and (12)

$$\frac{d^2u}{dl^2}+\left(\frac{2b}{a+bl}\right)\frac{du}{dl}+\beta^2u=0. \quad (13)$$

Solution of (13) following [12], and using (4)

$$\frac{Z_{in}}{Z(l)}=\frac{Z_a-jZ_1\left(\frac{b}{a\beta}+\tan\beta l\right)}{\left(\frac{b}{a\beta}\tan\beta l+1\right)Z_1+jZ_a\tan\beta l}+j\frac{b}{\beta\sqrt{Z}}.$$

VI. Conclusions

Equations that give the value of an arbitrary complex impedance transformed through a length of dissipationless, nonuniform line with an exponential, a cosine-squared and a parabolic taper were derived. The results should be useful in solving impedance matching problems in microwave circuits.

Acknowledgment

The author wishes to thank Dr. L. Young.

References

[1] C. R. Burrows, "The exponential transmission line," *Bell Syst. Tech. J.*, vol. 17, pp. 555–573, Oct. 1938.
[2] R. N. Ghose, "Exponential transmission lines as resonators and transformers," *IRE Trans. Microwave Theory Tech.*, vol. MTT-5, pp. 213–217, July 1957.
[3] D. Das and O. P. Rustogi, "Uniform transmission line equivalence of cascaded exponential lines," *IEEE Trans. Microwave Theory Tech.*, vol. MTT-16, pp. 511–516, Aug. 1968.
[4] C. P. Womack, "The use of exponential transmission lines in microwave components," *IRE Trans. Microwave Theory Tech.*, vol. MTT-10, pp. 124–132, Mar. 1962.
[5] A. Berquist, "Wave propagation on nonuniform transmission lines," *IEEE Trans. Microwave Theory Tech.*, vol. MTT-20, pp. 557–558, Aug. 1972.
[6] R. P. Arnold, W. L. Bailey, and R. L. Vaitkus, "Normalized impedance graphs for exponential transmission lines," *IEEE Trans. Microwave Theory Tech.*, vol. MTT-22, pp. 964–965, Nov. 1974.
[7] R. P. Arnold and W. L. Bailey, "Match impedances with tapered lines," *Electron. Des.* vol. 12; pp. 136–139, June 1974.
[8] H. Jasik, "Tapered lines," in *Antenna Engineering Handbook*. New York: McGraw-Hill, 1961, sect. 31.4.
[9] G. L. Ragan, *Microwave Transmission Circuits*. New York: McGraw-Hill, 1948, pp. 13–19.
[10] R. E. Collin, *Foundation for Microwave Engineering*. New York: McGraw-Hill, 1966, pp. 251–252.
[11] H. T. Davis, *Introduction to Nonlinear Differential and Integral Equations*. New York: Dover, 1962, pp. 59–62.
[12] D. A. Murray, *Introductory Course in Differential Equations*. London: Longmans, Green, 1958, pp. 114–117.

Green's Functions for Circular Sectors, Annular Rings, and Annular Sectors in Planar Microwave Circuits

RAKESH CHADHA, STUDENT MEMBER, IEEE,
AND K. C. GUPTA, SENIOR MEMBER, IEEE

***Abstract*—Green's functions for circular sector, annular ring, and annular sector shaped segments, in microwave planar circuits and microstrip antennas, have been derived in closed form.**

Manuscript received May 13, 1980; revised August 28, 1980. This work was supported by the Department of Electronics, Government of India.

The authors are with the Department of Electrical Engineering, Indian Institute of Technology, Kanpur-208016, India.

I. Introduction

Green's functions for the two-dimensional Helmholtz equation are used for the analysis of planar microwave circuits [1]. Two-dimensional microstrip antennas can also be analyzed using the Green's function method by finding voltages at various points along the periphery and calculating the radiation field from this voltage distribution [2]. The Green's functions for rectangular, circular, and triangular geometries are available [1], [3], [4]. Annular ring structures have been proposed for use in microstrip antennas [2], and are used in circuits like ratrace hybrids. The circular and annular sectors are encountered in microstrip bends as shown in Fig. 1, and their characterizations are needed for analyzing these bends accurately. Also, the characterization of an annular sector can be used to analyze accurately a tapered line segment, as shown in Fig. 2. However, the Green's functions for these geometries have not been reported so far. This article describes the development of Green's functions for annular rings and circular and annular sectors for which the sector angle is $180°/n$, where n is any positive integer.

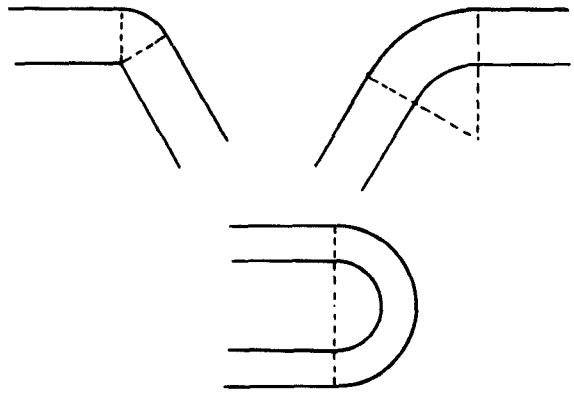

Fig. 1. Use of circular and annular sectors in stripline/microstrip bends.

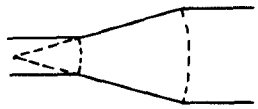

Fig. 2. A tapered line section modeled by an annular sector.

II. Planar Circuits

For planar circuits (Fig. 3), the Green's function G is given [1] by the solution of

$$(\nabla_T^2 + k^2)G = -j\omega\mu d\,\delta(\bar{r}-\bar{r}_0) \tag{1}$$

with

$$\frac{\partial G}{\partial n} = 0 \tag{2}$$

where n is the outward unit normal at any point on the periphery. In (1) above the time dependence of $\exp(-j\omega t)$ is assumed for all fields on the planar circuit.

The Green's function for any geometry can be obtained if the complete set of mutually orthogonal eigenfunctions for the given boundary conditions is known [5]. If $\psi_n(\bar{r})$ represent the normalized eigenunctions, then the Green's function can be expanded in terms of the eigenfunctions as

$$G(\bar{r}|\bar{r}_0) = j\omega\mu d \sum \frac{\psi_n^*(\bar{r}_0)\psi_n(\bar{r})}{k_n^2 - k^2} \tag{3}$$

where k_n^2 are the eigenvalues which satisfy

$$\nabla_T^2\psi_n + k_n^2\psi_n = 0 \tag{4}$$

and the superscript * denotes complex conjugate. For lossless circuits ψ_n are real and complex conjugate is not needed in (3). The Green's functions given by (3) contain an intrinsic singularity at $\bar{r}=\bar{r}_0$ but this singularity does not interfere with the determination of impedance matrices.

Solution of (1) gives Green's functions for both stripline type and microstrip type planar circuits shown in Fig. 3(a) and (b), respectively. In (2) a magnetic wall has been assumed at the periphery. The correction for fringing field would be different for stripline type and microstrip type planar circuits but with the magnetic wall assumed at the periphery the Green's functions are valid for both types of circuits.

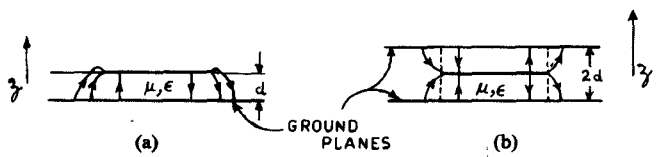

Fig. 3. Microstrip type and stripline type planar circuits.

III. Circular Sectors

For the circular sector shown in Fig. 4, the set of functions which satisfy the boundary conditions is given as

$$f_{m\nu}(\rho,\phi) = J_\gamma(k_{m\nu}\rho)\cos\gamma\phi \tag{5a}$$

where

$$\gamma = n\pi/\alpha \tag{5b}$$

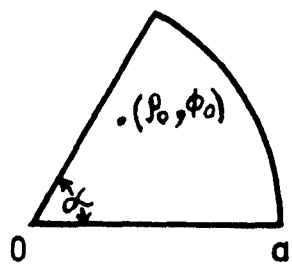

Fig. 4. A circular sector.

and $k_{m\nu}$ are chosen to satisfy

$$J_\gamma'(k_{m\nu}a) = 0. \tag{6}$$

In above, the subscript m is used to denote the mth root of (6), and n could be any nonnegative integer. In addition, m can take the value zero for $n=0$. This corresponds to $k_{m\nu}=0$ and implies that the function has a value of unity throughout the sector. The set of functions given by (5) are, in general, not orthogonal to each other. The functions are orthogonal if, and only if, ν is an integer which implies that π is an integral multiple of α.

Let us consider the case for which $\alpha=\pi/l$, where l is a positive integer. The set of functions discussed above are mutually orthogonal since ν takes only integral values. To obtain the Green's function using (3), these eigenfunctions must be normalized over the region of the sector. We have

$$\int_0^a J_{n_i}^2(k_{mn_i}\rho)\,d\rho = \begin{cases} a^2/2, & \text{if } m=\eta_i=0 \\ \text{else} & \frac{1}{2}\left[a^2 - \left(\eta_i^2/k_{mn_i}^2\right)\right]J_{n_i}^2(k_{mn_i}a) \end{cases} \tag{7}$$

where $\eta_i = nl$, and denotes that ν takes only integral values.

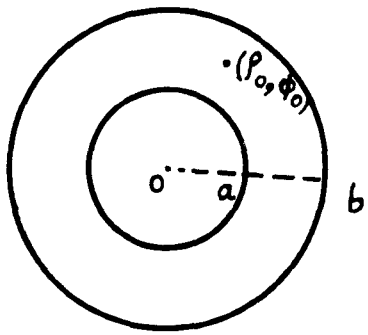

Fig. 5. An annular ring.

Using the normalization values given by (7), and those for $\cos(n_i\phi)$, the Green's function can be written as

$$G(\bar{r}|\bar{r}_0)=\frac{2ld}{j\omega\epsilon\pi a^2}+\sum_{n=0}^{\infty}\sum_{m=1}^{\infty}\frac{4lj\omega\mu d J_{n_i}(k_{mn_i}\rho_0)J_{n_i}(k_{mn_i}\rho)\cos n_i\phi_0\cos n_i\phi}{\epsilon_{n_i}\pi\left(a^2-\frac{n_i^2}{k_{mn_i}^2}\right)(k_{mn_i}^2-k^2)J_{n_i}^2(k_{mn_i}a)} \tag{8}$$

The angle of the sector α equals π/l, and $n_i=nl$. The eigenvalues $k_{mn_i}^2$ are given by

$$J_{n_i}'(k_{mn_i}a)=0 \tag{9}$$

and

$$\epsilon_{n_i}=\begin{cases}2, & \text{if } n_i=0\\ 1, & \text{if } n_i>0.\end{cases} \tag{10}$$

For $l=1$, when the sector reduces to a semicircle the Green's function is same as the even mode Green's function of a circle. Thus the Green's function given by (8) is consistent with the Green's function for a circle [3].

IV. Annular Rings

For the annular ring structure shown in Fig. 5, the set of mutually orthogonal eigenfunctions which satisfy the boundary condition (3), on the periphery is given by

$$f_{mn}(\rho,\phi)=[N_n'(k_{mn}a)J_n(k_{mn}\rho)-J_n'(k_{mn}a)N_n(k_{mn}\rho)]\begin{Bmatrix}\cos n\phi\\ \sin n\phi\end{Bmatrix} \tag{11}$$

where the eigenvalues k_{mn} are obtained from

$$\frac{J_n'(k_{mn}a)}{N_n'(k_{mn}a)}=\frac{J_n'(k_{mn}b)}{N_n'(k_{mn}b)}. \tag{12}$$

As in (6), in the above equation also, n takes nonnegative integral values and m takes positive integral values. In addition m can take the value zero for $n=0$, which corresponds to a unity value throughout the region and $k_{mn}=0$.

To obtain the Green's function using (3), the eigenfunctions described by (11) are normalized. We use

$$\int_a^b\rho[N_n'(k_{mn}a)J_n(k_{mn}\rho)-J_n'(k_{mn}a)N_n(k_{mn}\rho)]^2\,d\rho=\frac{1}{2}\left[\left(b^2-\frac{n^2}{k_{mn}^2}\right)\{N_n'(k_{mn}a)J_n(k_{mn}b)-J_n'(k_{mn}a)N_n(k_{mn}b)\}^2-\left(a^2-\frac{n^2}{k_{mn}^2}\right)\{N_n'(k_{mn}a)J_n(k_{mn}a)-J_n'(k_{mn}a)N_n(k_{mn}a)\}^2\right] \tag{13}$$

and usual normalizing relations for $\cos n\phi$ and $\sin n\phi$. The Green's function for the annular ring can now be written as

$$G(\bar{r}|\bar{r}_0)=\frac{d}{j\omega\epsilon\pi(b^2-a^2)}+\sum_{n=0}^{\infty}\sum_{m=1}^{\infty}\frac{2j\omega\mu d F_{mn}(\rho_0)F_{mn}(\rho)\cos[n(\phi-\phi_0)]}{\epsilon_n\pi\left[\left(b^2-\frac{n^2}{k_{mn}^2}\right)\{F_{mn}(b)\}^2-\left(a^2-\frac{n^2}{k_{mn}^2}\right)\{F_{mn}(a)\}^2\right](k_{mn}^2-k^2)} \tag{14}$$

where $F_{mn}(\rho)$ is defined as

$$F_{mn}(\rho)=N_n'(k_{mn}a)J_n(k_{mn}\rho)-J_n'(k_{mn}a)N_n(k_{mn}\rho) \tag{15}$$

and k_{mn} are chosen to satisfy (12). To use this Green's function for analyzing an annular ring, (12) has to be solved repeatedly to obtain k_{mn}'s.

V. Annular Sectors

The Green's functions for annular sectors (shown in Fig. 6) can be obtained in the same way as for circular sectors. The set of functions which satisfy the boundary conditions is given by

$$f_{m\nu}(\rho,\phi)=[N_\nu'(k_{m\nu}a)J_\nu(k_{m\nu}\rho)-J_\nu'(k_{m\nu}a)N_\nu(k_{m\nu}\rho)]\cos\nu\phi \tag{16}$$

where $\nu=n\pi/\alpha$, and $k_{m\nu}$ satisfy

$$\frac{J_\nu'(k_{m\nu}a)}{N_\nu'(k_{m\nu}a)}=\frac{J_\nu'(k_{m\nu}b)}{N_\nu'(k_{m\nu}b)}. \tag{17}$$

These functions are mutually orthogonal if, and only if, $\alpha=\pi/l$, where l is a positive integer. The Green's function can now be written as

$$G(\bar{r}|\bar{r}_0)=\frac{2ld}{j\omega\epsilon\pi(b^2-a^2)}+\sum_{n=0}^{\infty}\sum_{m=1}^{\infty}\frac{4lj\omega\mu d F_{mn_i}(\rho_0)F_{mn_i}(\rho)\cos n_i\phi_0\cos n_i\phi}{\epsilon_{n_i}\pi\left[\left(b^2-\frac{n_i^2}{k_{mn_i}^2}\right)F_{mn_i}^2(b)-\left(a^2-\frac{n_i^2}{k_{mn_i}^2}\right)F_{mn_i}^2(a)\right](k_{mn_i}^2-k^2)}. \tag{18}$$

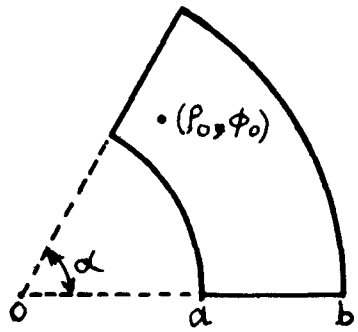

Fig. 6. An annular sector.

The angle of the sector is $\alpha = \pi/l$, and $n_i = nl$. The function $F_{mn_i}(\rho)$ is given by (15) and k_{mn_i} are obtained by solving (17). It can be seen that this Green's function is consistent with the Green's function for the annular ring in the same way as the Green's function for a circular sector is with that of a circle.

Using the Green's functions given by (8), (14), and (18), the Green's function technique of analyzing planar circuits and microstrip antennas can be extended to circuits incorporating circular sectors, annular rings and annular sectors. These Green's functions are valid both for triplate stripline type circuits and for open microstrip type circuits.

References

[1] T. Okoshi and T. Miyoshi, "The planar circuit—An approach to microwave integrated circuitry," *IEEE Trans. Microwave Theory Tech.*, vol. MTT-20, pp. 245–252, Apr. 1972.

[2] Y. T. Lo, D. Solomon, and W. F. Richards, "Theory and experiment on microstrip antennas," *IEEE Trans. Antennas Propagat.*, vol. AP-27, pp. 137–145, Mar. 1979.

[3] T. Okoshi, T. Takeuchi, and J. P. Hsu, "Planar 3-db Hybrid Circuit," *Electron. Commun. Japan*, vol. 58-B, no. 8, pp. 80–90, Aug. 1975.

[4] R. Chadha and K. C. Gupta, "Green's functions for triangular segments in planar microwave circuits," *IEEE Trans. Microwave Theory Tech.*, vol. MTT-28, pp. 1139–1143, Oct. 1980.

[5] P. M. Morse and H. Feshbach, *Methods of Theoretical Physics*. New York: McGraw-Hill, 1953, ch. 7, p. 820.

Segmentation Method Using Impedance Matrices for Analysis of Planar Microwave Circuits

RAKESH CHADHA, STUDENT MEMBER, IEEE,
AND K. C. GUPTA, SENIOR MEMBER, IEEE

***Abstract*—Segmentation method for the analysis of two-dimensional microwave planar circuits is modified by using *Z*-matrices for the individual planar segments. The proposed method is compared with the previously reported method using *S*-matrices and is shown to be computationally more efficient.**

Manuscript received June 9, 1980; revised September 2, 1980. This work was supported by the Department of Electronics, Government of India.

The authors are with the Department of Electrical Engineering, Indian Institute of Technology, Kanpur 208016, India.

I. Introduction

Two-dimensional microwave planar circuits have been proposed for use in microwave integrated circuits [1]. One of the methods, for analyzing planar components, involves determination of *Z*-matrix of the component using Green's functions. The Green's functions are available for only a few regular shapes. Analysis of other shapes is normally done by segmenting these into shapes for which the Green's functions are known. The Segmentation Method [2], [3] uses this approach and combines the *S*-matrices of the individual components to obtain overall *S*-matrix. A formulation for combining segments to form 2-port and 4-port circuits is given in [2], [3] and could be extended to any general *n*-port network.

In this method a considerable effort is spent in computing *S*-matrices for each of the segments. These matrices are then combined to obtain the overall *S*-matrix. Considerable reduction in computational effort can be achieved if *Z*-matrices of individual components are combined to give the overall *Z*-matrix from which the overall network scattering matrix may be determined. A segmentation method that combines *Z*-matrices of the segments is described in this article.

II. Segmentation Using *S*-Matrices

In the segmentation method using *S*-matrices, we proceed as follows. The *S*-matrices for the individual segments are put together as [4]

$$\begin{bmatrix} \bar{b}_p \\ \bar{b}_c \end{bmatrix} = \begin{bmatrix} \tilde{S}_{pp} & \tilde{S}_{pc} \\ \tilde{S}_{cp} & \tilde{S}_{cc} \end{bmatrix} \begin{bmatrix} \bar{a}_p \\ \bar{a}_c \end{bmatrix} \tag{1}$$

where $\bar{a}_p$ $\bar{b}_p$ and $\bar{a}_c$, $\bar{b}_c$ are the normalized wave variables at the p external and c internal connected ports. The interconnection constraints are given as

$$\bar{b}_c = \tilde{\Gamma}\bar{a}_c \tag{2}$$

where $\tilde{\Gamma}$ is the connection matrix. The overall *S*-matrix is obtained as

$$\tilde{S}_p = \tilde{S}_{pp} + \tilde{S}_{pc}\left(\tilde{\Gamma} - \tilde{S}_{cc}\right)^{-1}\tilde{S}_{cp}. \tag{3}$$

The solution of (3) requires inversion of a matrix of order equal to the number of interconnected ports. Let us consider an example shown in Fig. 1 to illustrate the total computational effort needed in the segmentation method. This network is a planar circuit version of a compensated in-line power divider [5]. Segment B, and C_1 and C_2 parts of segment C are quarter-wave transformers with characteristic impedances equal to $Z_0/(2^{1/4})$ and $(2^{1/4})Z_0$, respectively. Segments A, D, and E are portions of outgoing transmission lines (characteristic impedance Z_0). These three segments are considered as planar components in order to take into account any higher order modes that may be excited by the discontinuities present at the ends of three transformers. For better accuracy, each external port is divided into six subports for obtaining the *Z*-matrix. The six subports are combined together using ideal six-way power dividers (not shown in the figure) at each external port [3]. To obtain *S*-matrices of individual segments, five complex matrices, three of order 12 and one each of order 14 and 20, are to be inverted. The number of interconnections in the network is now 44 and so a complex matrix of order 88 has to be inverted to obtain the overall scattering matrix.

0018-9480/81/0100-0071$00.75 ©1981 IEEE